Stem Cell Reports
Article

ISSCR

OPEN ACCESS

# Human primed and naïve PSCs are both able to differentiate into trophoblast stem cells

Sergey Viukov,[1] Tom Shani,[1] Jonathan Bayerl,[1] Alejandro Aguilera-Castrejon,[1] Bernardo Oldak,[1] Daoud Sheban,[1] Shadi Tarazi,[1] Yonatan Stelzer,[2] Jacob H. Hanna,[1,*] and Noa Novershtern[1,*]

[1]Department of Molecular Genetics, Weizmann Institute of Science, Rehovot 7610001, Israel
[2]Department of Molecular Cell Biology, Weizmann Institute of Science, Rehovot 7610001, Israel
*Correspondence: jacob.hanna@weizmann.ac.il (J.H.H.), noa.novershtern@weizmann.ac.il (N.N.)
https://doi.org/10.1016/j.stemcr.2022.09.008

## SUMMARY

The recent derivation of human trophoblast stem cells (TSCs) from placental cytotrophoblasts and blastocysts opened opportunities for studying the development and function of the human placenta. Recent reports have suggested that human naïve, but not primed, pluripotent stem cells (PSCs) retain an exclusive potential to generate TSCs. Here we report that, in the absence of WNT stimulation, transforming growth factor β (TGF-β) pathway inhibition leads to direct and robust conversion of primed human PSCs into TSCs. The resulting primed PSC-derived TSC lines exhibit self-renewal, can differentiate into the main trophoblast lineages, and present RNA and epigenetic profiles that are indistinguishable from recently established TSC lines derived from human placenta, blastocysts, or isogenic human naïve PSCs expanded under human enhanced naïve stem cell medium (HENSM) conditions. Activation of nuclear Yes-associated protein (YAP) signaling is sufficient for this conversion and necessary for human TSC maintenance. Our findings underscore a residual plasticity in primed human PSCs that allows their *in vitro* conversion into extra-embryonic trophoblast lineages.

## INTRODUCTION

The mammalian placenta is an organ that mediates interaction between mother and fetus. It supplies the fetus with nutrients and oxygen, secretes hormones, and controls maternal tissue remodeling and, thus, ensures normal pregnancy progression (Turco and Moffett, 2019). Cells of the trophoblast lineage, constituting significant part of the placenta, originate from the trophectoderm (TE), an outer layer of the preimplantation embryo (James et al., 2012). Segregation of the TE from the inner cell mass (ICM) establishes the earliest cell fate decision in the developmental time course (Niakan et al., 2012).

At embryo implantation stages, trophoblast cells penetrate the endometrium and subsequently form the scaffold of placental villi (Figure 1A; Latos and Hemberger, 2016). The inner part of this scaffold consists of undifferentiated mononuclear cytotrophoblast (CT) cells, which proliferate and can differentiate into two main types of trophoblast lineage. First, fused CT cells form the outermost layer of the villi, multinuclear syncytium trophoblast (STB), which ensures nutrient exchange between the fetus and the mother. These cells also secrete hormones like chorionic gonadotropin (hCG) and progesterone. Second, extravillous trophoblasts (EVT), which originates from CT cells positioned at the tip of the villi. The latter cells penetrate the endometrium and maternal blood vessels, remodeling the latter (James et al., 2012). One of the important regulators of the trophoblast lineage specification is nuclear YAP (Yes-associated protein) signaling. It is a key trigger for TE specification of the outer cells of early blastocyst in the mouse (Rossant and Tam, 2009) and human (Gerri et al., 2020). Later in human development, it supports proliferation and expression of stemness genes in CT cells and prevents their differentiation (Meinhardt et al., 2020).

Derivation of trophoblast stem cells (TSCs) from the first-trimester placenta or blastocysts provides an opportunity to study aspects of placental development and function *in vitro* (Okae et al., 2018). Particularly, TSCs derived from human naïve induced pluripotent stem cells (iPSC) from different genetic backgrounds can help model placental developmental complications. Naïve embryonic stem cells model the ICM cells of preimplantation blastocyst (Ying et al., 2008), whereas primed embryonic stem cells model early post-implantation epiblast (Weinberger et al., 2016). These two cell states can be maintained indefinitely *in vitro* and can be inter-converted by changing the growth conditions, affecting several aspects, such as X chromosome reactivation and the ability to contribute to chimeras (Bayerl et al., 2021; Gafni et al., 2013; Guo et al., 2017).

Conversion of human pluripotent stem cells (hPSCs) into TSCs was first achieved *in vitro* from naïve hPSCs by applying TSC maintenance medium (Cinkornpumin et al., 2020; Dong et al., 2020; Guo et al., 2021; Io et al., 2021; Liu et al., 2020), but not from the primed hPSC state. This is in line with the ability to convert mouse naïve, but not primed, embryonic stem cells to mouse TSCs (Blij et al., 2015) and is regarded as a reflection of developmental proximity between mammalian ICM (modeled by naïve embryonic stem cells [ESCs]) and the trophoblast lineage. These studies have promoted the notion that TSC

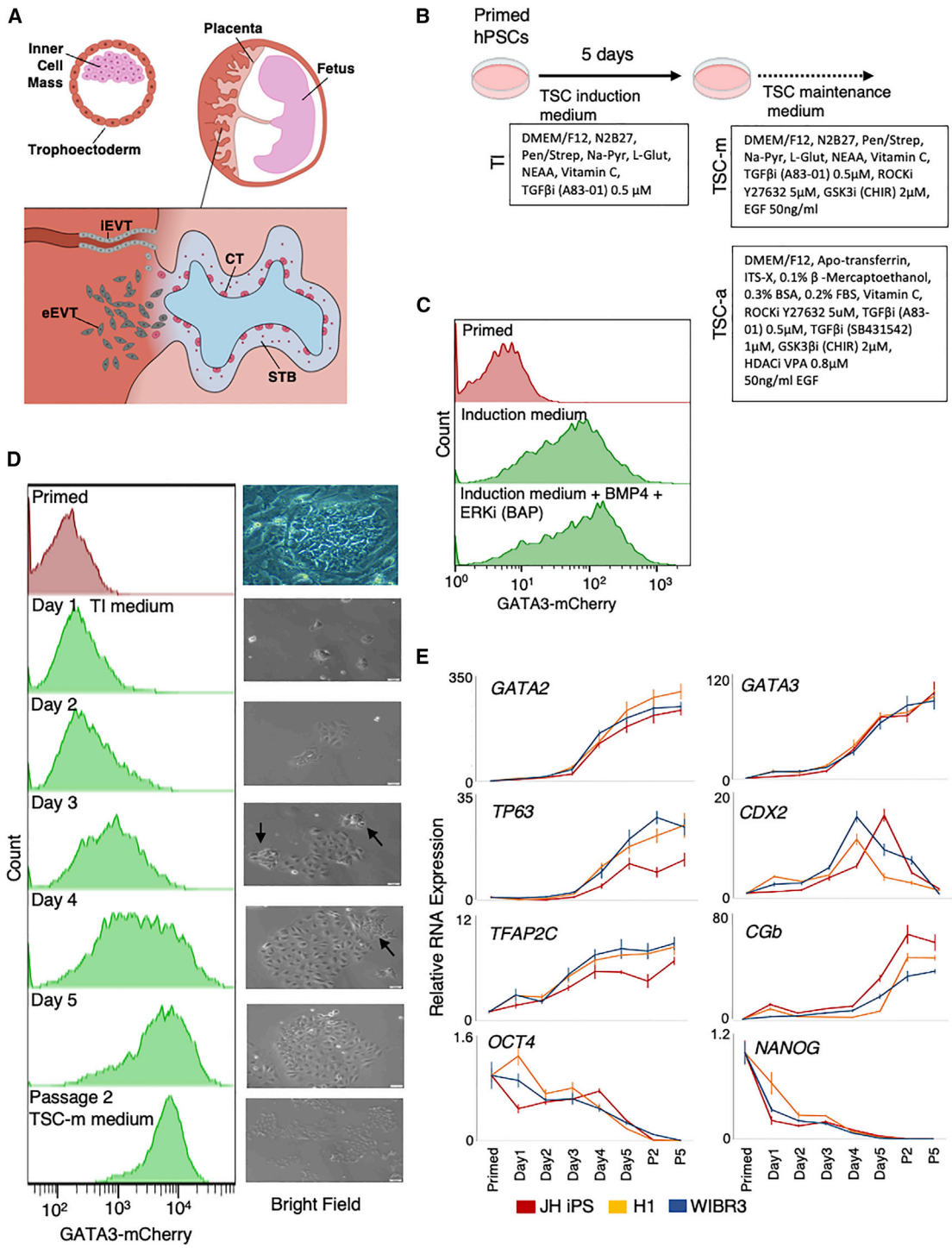


**Figure 1. TSC markers are upregulated after TSC induction of primed hPSCs**

(A) The placenta is developed from trophectoderm (TE). The inner part of the placenta villi consists of cytotrophoblast (CT), which can fuse and generate syncytiotrophoblast (STB) or exit the villi to generate extravillous trophoblasts (EVT), which penetrates the endometrium (eEVT) and maternal blood vessels (iEVT).

(B) Experimental flow. Human primed pluripotent stem cells (ESCs and iPSCs) were maintained in TI medium for 5 days and then transferred into TSC-a or TSC-m medium.

*(legend continued on next page)*

differentiation potential is retained exclusively in human naïve, but not primed, PSCs (Guo et al., 2021).

A recent report (Mischler et al., 2021) described conversion of hPSCs grown in E8 medium into TSCs. Other works (Jang et al., 2022; Soncin et al., 2022; Wei et al., 2021) describe direct conversion of human primed PSCs to TSCs by BMP4 stimulation, whereas establishment of stable cultures took at least 5 passages or involved subcloning. However, no work has compared, side by side, conversion from isogenic naïve and primed PSCs. The molecular and signaling bases of such differences in TSC differentiation competence from these two cell states have not been resolved so far. Finally, no TSC induction protocol has been shown to be rapid, robust, and working on multiple cell lines, regardless of their naïve or primed pluripotency origin.

Here we report a protocol for direct and robust conversion of primed hPSCs from multiple genetic backgrounds into TSC cell lines sharing properties, transcription, and chromatin profiles with human placenta or naïve PSC-derived TSCs. We found that inhibition of transforming growth factor β (TFG-β) pathway is necessary and sufficient to achieve this conversion. We also found that addition of the GSK3 inhibitor CHIR99021 (CHIR) inhibits this conversion in primed PSCs. We also show that activation of YAP, the major factor of the Hippo signaling pathway, can replace TGF-β inhibition in the conversion protocol, whereas *YAP* knockout hPSCs can show some upregulation of TSC markers but fail to proliferate, making YAP sufficient for this conversion and indispensable for human TSC maintenance.

## RESULTS

### Derivation of TSC lines from primed hPSCs

To study conversion of primed/conventional human ESC (hESC) and hiPSC lines into the trophoblast lineage, a reporter for *GATA3* expression, which is highly expressed in TE and in the first-trimester placenta (Petropoulos et al., 2016; Soncin et al., 2018), was generated using a CRISPR-Cas9 strategy (Figures S1A–S1C). The P2A-mCherry reporter was inserted at the 3′ end of the *GATA3* coding sequence in the WIBR3 hESC line, which was maintained in primed conditions (Table S1) from the moment of derivation (Lengner et al., 2010). We then attempted to induce these human primed GATA3 reporter cells (W3GC) to become TSCs on Matrigel coated plates, using TSC induction (TI) medium we optimized in this study, which includes N2B27 and TGF-β inhibitor (A83-01; Table S1). Three days after seeding these cells in TI medium (Figure 1B), the GATA3 reporter was robustly upregulated (Figure 1C), suggesting trophoblast program induction. A conventional, previously established way of differentiating hPSCs into the trophoblast lineage involves using "BAP" conditions (BMP4, TGF-β inhibitor A83-01, ERK inhibitor PD0325901) (Amita et al., 2013). In our system, there was no significant difference in GATA3 reporter induction between TI medium and BAP conditions (Figure 1C).

Next, primed W3GC hESCs, H1 hESCs, and JH iPSCs were seeded into TI medium, and expression of trophoblast markers was monitored daily. mCherry upregulation was apparent 24 h after induction in W3GC, and by day 5, more than 90% of the cells expressed it at a high level (Figure 1D). Additional trophoblast markers, like *GATA2*, *TP63*, *TFAP2C*, *CDX2*, and *CGB*, gradually increased, and the pluripotent markers *OCT4* and *NANOG* decreased during 5 days of induction (Figure 1E), indicating that the cells were effectively converted to the trophoblast lineage and lost their pluripotency. The morphology of the cells also changed gradually. For example, by day 4 (Figure 1D, right panel), most of the cells have already acquired a cobblestone, flattened, TSC-like appearance, whereas some small groups of cells still looked more like primed hESCs. By day 5, the latter cells were not visible. Despite not using a ROCK inhibitor in this experiment, we did not notice significant cell death in the cultures, and the colonies rapidly increased in size.

After 5 days in TI medium, the cells grew confluent and were passaged to Collagen-IV-coated plates into TSC maintenance (TSC-m) medium (including N2B27, A83-01, epidermal growth factor (EGF), the GSK3 inhibitor CHIR, and the ROCK inhibitor Y27632; Table S1). After one or two passages in TSC-m medium, all cells showed homogeneous TSC morphology and GATA3 expression (Figure 1D), whereas TSC markers persisted in their induction (Figure 1E). One interesting exception was *CDX2*, which peaked around day 5 of induction of primed hPSCs and then was repressed by passages 1–2. This is in line with a previous report (Guo et al., 2021), according to which

(C) Levels of the GATA3-mCherry reporter, as measured in the W3GC hESC line, maintained under primed conditions (top panel), 3 days after seeding in TI medium (center panel), or in TI medium + BMP4 + ERK inhibitor (BAP conditions).
(D) Left: levels of the GATA3-mCherry reporter, as measured in the primed W3GC hESC line, during maintenance in TI medium for 5 days and after passage in TSC-m medium. Right: bright-field image of the cell culture at the indicated time points. Arrows indicate cells with hESC-like morphology remaining in culture at days 3–4.
(E) Expression of selected markers in cells maintained in TI medium for 5 days and in TSC-m medium for 2 and 5 passages. Cells lines are human iPSCs and human ESCs (H1 and WIBR3). n = 3 independent experiments.

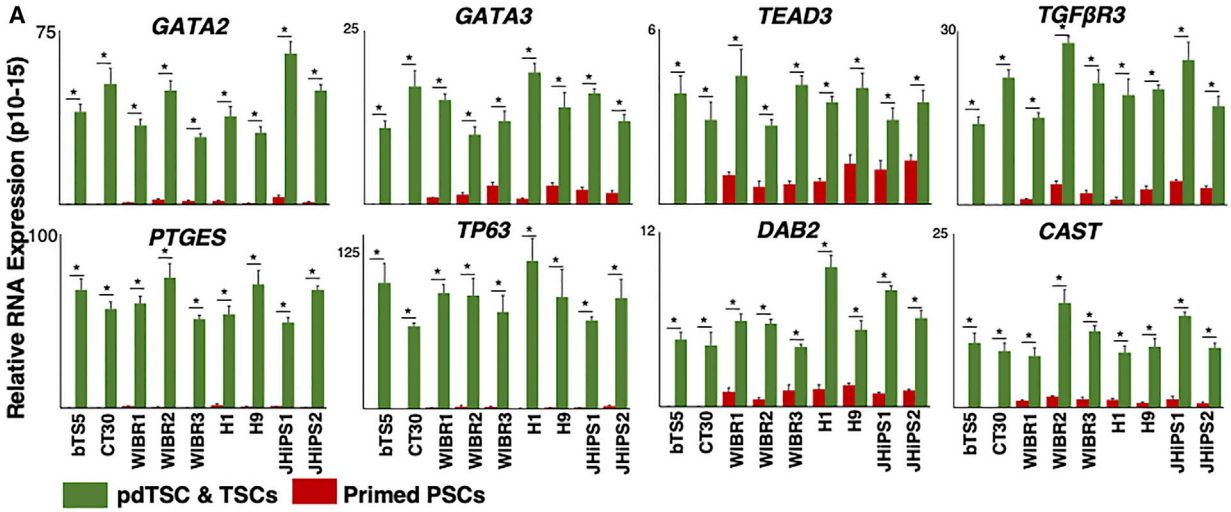


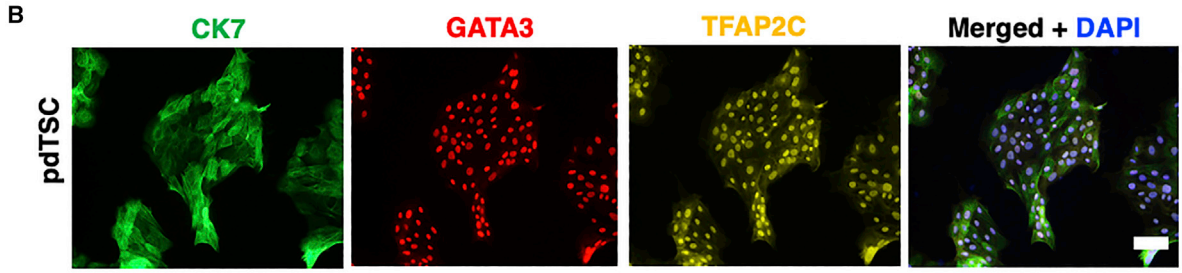


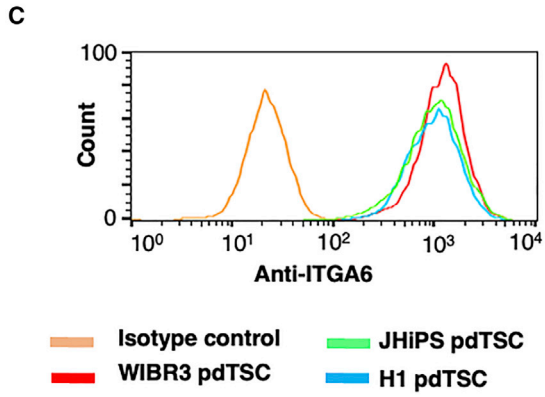


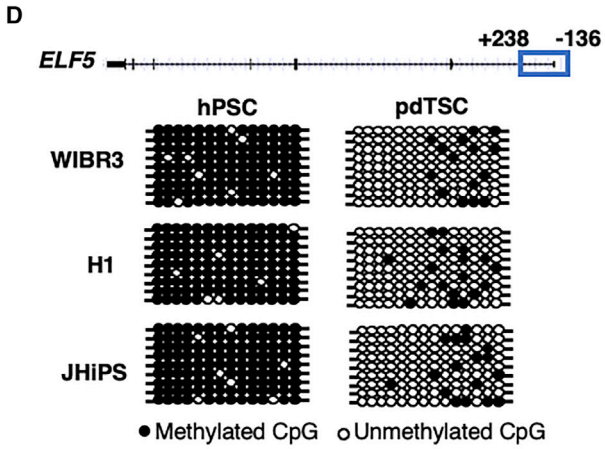


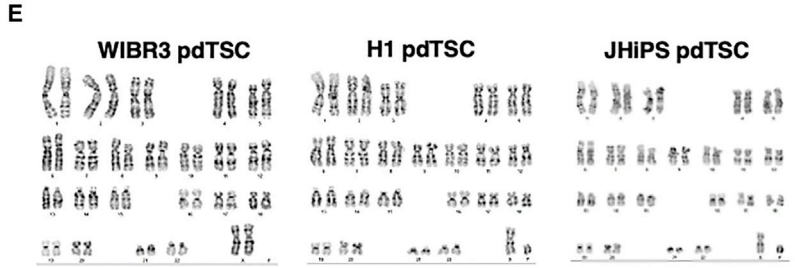


F

**HENSM**

FGFRi/MEKi (PD0325901 1-1.2μM*)
PKCi (Go6983 2μM)
WNTi (XAV939 2μM)
SRCi (CGP77675 1μM)
LIF (10 ng/ml)
ACTIVIN A (5 ng/ml)
ROCKi (Y27632 1.2μM)

*(legend on next page)*

*CDX2* is similarly transiently upregulated during naïve hPSC-to-TSC conversion and, so far, cannot be maintained in any previously described human TSC lines. To test different durations of TI medium usage (Figure S1D), W3GC cells were induced for 2–9 days and then grown in TSC-m medium for 2 passages. The optimal duration of TI medium was found to be 5–6 days, whereas shorter or longer induction periods result in a significant increase in mCherry-negative cells.

The TSC state remained stable after prolonged passaging of all derived lines. High expression of trophoblast markers was detected by RT-PCR after 10–15 passages in TSC-m medium (Figure 2A). Cells were stained positively for TFAP2C, GATA3, and KRT7 (CK7 protein) after 15 passages (Figure 2B), and the trophoblast marker ITGA6 was also highly expressed, as detected by fluorescence-activated cell sorting (FACS) (Figure 2C). Cells could be kept for at least 30 passages without changes in their morphology and markers, showing no changes in cell identity (Figures S2A and S2B). Using the same protocol, we converted to TSCs other published primed/conventional hPSC lines that have never been maintained under anything other than primed conditions (H9, WIBR1, and WIBR2). These TSC lines have shown the same morphology and marker expression as the ones converted from the WIBR3 background and as TSC lines derived from human placenta and blastocyst (Figures 2A and S2C), indicating that the identity of TSCs obtained *in vitro* is independent in the genetic background of the cells. These results exclude the possibility that the ability to obtain TSCs from primed hPSCs is a sporadic and/or cell-specific phenomenon. We labeled the cells as primed-state-derived TSCs (pdTSCs).

We next moved to conduct in-depth validation of pdTSCs. Demethylation of the *ELF5* promoter is considered to be an important marker of human TSCs (Hemberger et al., 2010; Okae et al., 2018). The methylation status of the *ELF5* promoter was estimated in three pdTSC lines and in their parental primed hPSCs. Although the *ELF5* promoter was highly methylated in hPSCs (>94% methylation), methylation was lost in all pdTSCs measured (Figure 2D). The karyotype of pdTSCs remained stable even after 20–25 passages with no apparent chromosomal aberrations (Figure 2E).

The TSC-m medium described here is similar to conditions that have been described previously (TSC-a; Okae et al., 2018; Table S1; Figure 1B) but lacks an HDAC inhibitor (VPA) and is based on B27, whereas the conventional growth medium contains a low concentration of fetal bovine serum (FBS). We could similarly derive pdTSCs from the same primed hPSCs by using the TSC-a medium described previously by Okae et al. (2018). When comparing the pdTSCs expanded in TSC-m and TSC-a medium conditions, similar marker expression was detected (Figure S2C), but TSC-a cells had lower growth rate (Figure S2D) and higher expression of EVT and STB differentiation markers (*HLA-G* and *CGB*, respectively; Figure S2E). Cell cycle mitotic genes were upregulated in RNA sequencing (RNA-seq) from cells induced in TSC-m compared with TSC-a, indicating a higher mitotic rate (Figures S2G and S2F). Thus, for routine maintenance, TSC-m conditions were used in this study.

## pdTSC lines share a transcriptional profile and chromatin configuration with other TSC lines

Consistent with previous papers (Cinkornpumin et al., 2020; Dong et al., 2020; Io et al., 2021), naïve hPSCs expanded under optimized and standardized human enhanced naïve stem cell medium (HENSM) conditions (Bayerl et al., 2021; Figure 2F; Table S1), generated TSC lines, called ndTSCs (naïve-state-derived TSCs), from multiple cell lines (H1, WIBR3, and JH iPSC).

Next, RNA-seq profiles of H1- and WIBR3-derived pdTSCs and ndTSCs were compared with previously described embryo-derived TSC (edTSC) lines derived from human blastocyst and first-trimester placenta (Okae et al., 2018). All lines were maintained under TSC-m and TSC-a

**Figure 2. Cells retain TSC identity after a prolonged time**

(A) Expression of trophoblast markers as measured by RT-PCR in pdTSCs that were maintained for a prolonged time (10–15 passages) in TSC-m medium or in primed hPSCs compared with the native TSC lines bTS5 and CT30. Student's t test, *$p < 0.05$. n = 5 independent experiments.

(B) Immunostaining of the trophoblast markers CK7, GATA3, and TFAP2C in pdTSCs that were maintained for a prolonged time (15 passages) in TSC-m medium.

(C) FACS analysis of H1, WIBR3, and JH iPSC pdTSCs, measuring anti-ITGA6 or immunoglobulin G (IgG) (negative control), after 15 passages in TSC-m medium.

(D) Methylation levels of the *ELF5* promoter, as measured in the indicated primed hPSC lines (left) and in their derived pdTSCs (right).

(E) Karyotype analysis for H1, JH iPSC and WIBR3 pdTSCs, indicating a normal karyotype.

(F) Summary of cytokines and small-molecule inhibitors used under optimized and standardized HENSM conditions for induction and maintenance of human naïve PSCs (as detailed in Table S1). *Some hPSC lines required slightly higher inhibition of FGF/MEK/ERK signaling to achieve a more homogeneous, dome-like morphology, which could be done by increasing MEKi/ERKi (PD0325901) from 1 μM to 1.2 μM or simply adding 0.05–0.1 μM FGFRi (PD173074) to the medium.

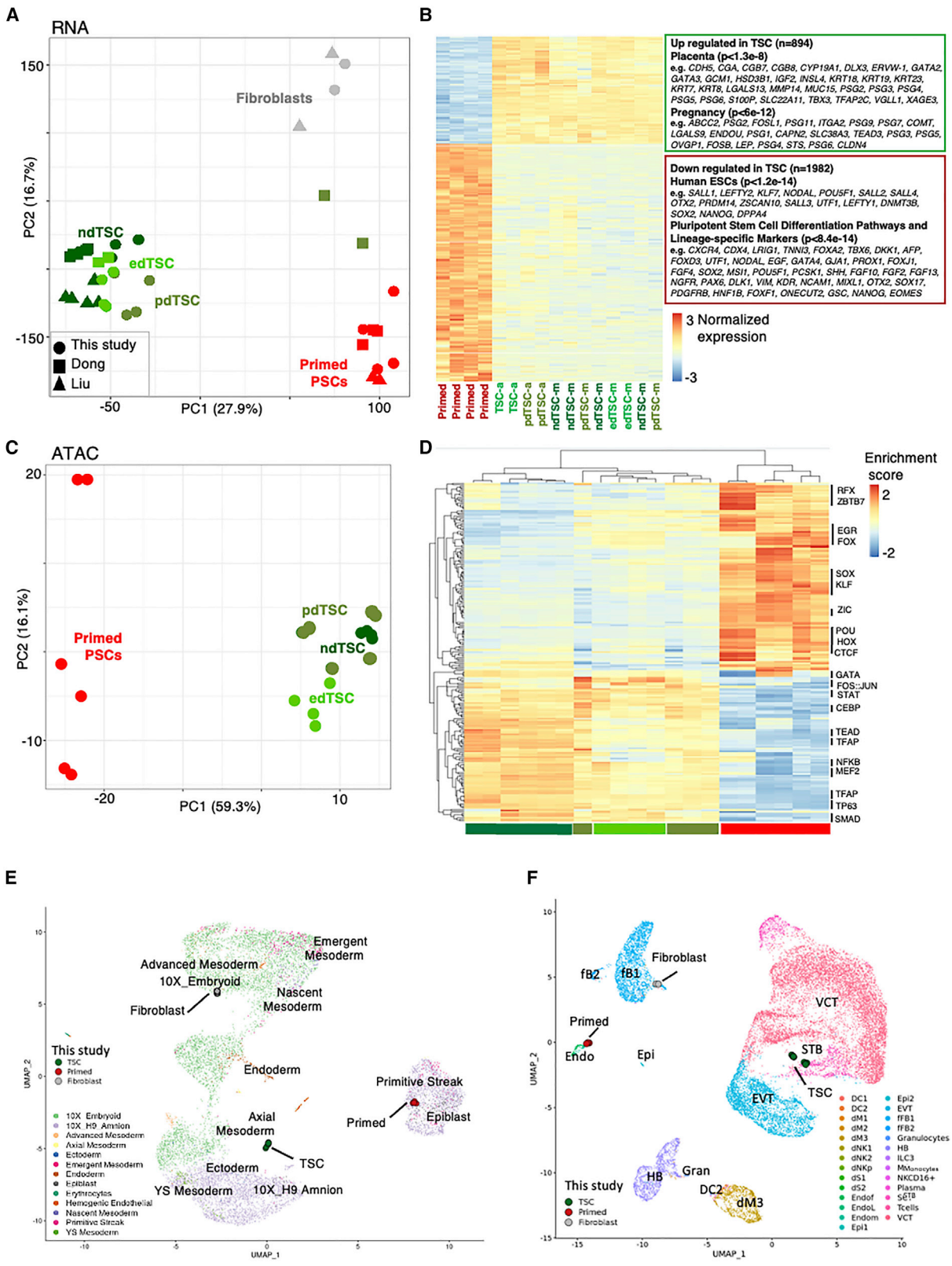


*(legend on next page)*

conditions. Profiles were compared with primed hPSCs, human fibroblasts, and previously published ndTSC and hPSC samples (Dong et al., 2020; Liu et al., 2020). All TSC lines clustered together and separately from hPSCs and fibroblasts (Figure 3A), showing the transcriptional difference between derived TSCs and other cell types. The main transcriptional differences that were observed between TSCs of different origin were those between TSC-a or TSC-m medium (Figure S3A), supporting our previous findings (Figures S2C–S2F). Overall, 894 genes were upregulated in TSCs compared with hPSCs and were highly enriched for placental genes, including well-known TSC markers such as *GCM1*, *CGA*, *CGB5*, *ERVFRD-1*, *KRT7*, *GATA2*, *GATA3*, and *ELF5* (Figures 3B and S3B). Canonical pluripotency genes such as *OCT4*, *SOX2*, *NANOG*, and *DPPA4* were downregulated in all TSCs as expected (Figures 3B and S3B).

Next, chromatin configuration was measured in TSC and hPSC samples using ATAC-seq. Motif enrichment analysis of open chromatin regions clustered the samples into distinct clusters (Figure 3C), showing that the difference between TSCs and other cell types is robust and rewired in the chromatin configuration. The top motifs that are associated with all TSC samples include known TSC regulator families such as GATA, TFAP, TEAD, CEBP and FOS-JUN, and the top motifs that are associated with hPSC samples include OCT4 (POU), SOX, and KLF (Figure 3D). Both observations are well coordinated with the expression and function of these transcription factors (Figure S3B).

A recent pre-print (Zhao et al., 2021) has described principles and markers to be used to avoid confusion between identifying placental versus amniotic cells. To rule out the possibility that our pdTSCs are amniotic, their RNA-seq profiles were projected on reference single-cell RNA-seq datasets (Tyser et al., 2021; Zheng et al., 2019). Although fibroblasts and primed hESCs were projected on their corresponding *in vivo* counterparts (Figure 3E), pdTSCs were not projected on amnion cells. Amnion markers such as *BAMBI*, *ISL1*, and *IGFBP3* were not upregulated in pdTSCs compared with edTSCs or primed hPSCs (Figure S3C), ruling out the possibility that the cells are amniotic. When samples were projected on *in vivo* placental single-cell RNA-seq (Vento-Tormo et al., 2018), TSCs were clustered with TSC-driven cells (STB, EVT, and villous CT [VCT]) and away from fibroblasts and immune and endothelial cells (Figure 3F).

A recent report (Guo et al., 2021) indicated that exposure of human primed hPSCs to medium containing TGF-β and ERK pathway inhibitors results in upregulation of amnion markers, whereas *GATA3* and other trophoblast marker expression remains low. Testing amnion and trophoblast marker expression in primed hPSCs induced with TI medium (containing the TGF-β inhibitor A83-01) or TI medium + ERK inhibitor (Figure S3D), we observed transient induction of amnion markers by day 5 under both conditions (Dong et al., 2020), followed by a decrease to basal levels after 2 passages in TSC-m medium. The latter might suggest that hPSCs induced to become pdTSCs transiently initiate a partial amnion-like program that is quickly repressed upon maturation of the TSC phenotype or that the induction phase simultaneously generates TSCs and a small fraction of amnion cells that are later lost as the culture becomes dominated by the established pdTSCs. Trophoblast markers and the *GATA3*-mCherry reporter were robustly induced under both conditions (Figures S3D and S3E). Overall, these results show that pdTSCs share transcriptional and chromatin profiles with previously published ndTSCs, with edTSCs derived directly from the placenta, and with *in vivo* sampled

**Figure 3. The pdTSC transcriptional profile is nearly indistinguishable from previously derived TSCs**

(A) Principal component analysis of RNA-seq profiles from pdTSCs, ndTSCs, edTSCs, primed hPSCs, and fibroblasts alongside previously published datasets (Dong et al., 2020; Liu et al., 2020), showing that pdTSCs cluster with ndTSCs and edTSCs from the different datasets and that all are separated from hPSCs or fibroblasts. pdTSCs and ndTSCs were derived from H1 and WIBR3 primed and naïve cells. For naïve lines, the derivation was performed by direct application of TSC-m medium with or without an induction step, as detailed in Table S2.

(B) Differentially expressed genes between edTSCs/pdTSCs/ndTSCs and primed hPSCs. 894 genes were upregulated in TSCs, enriched for placenta-related gene signatures. 1,981 genes were downregulated in TSCs, enriched for ESC gene signatures. Selected genes are highlighted. The complete DEG lists and enrichment are available in Table S3.

(C) Principal-component analysis of pdTSC, ndTSC, edTSC, and naïve and primed hPSC samples, based on motifs enriched in accessible chromatin regions (ChromVar), showing that pdTSCs cluster with TSCs away from primed hESCs.

(D) Motif enrichment in ndTSC, pdTSC, edTSC, and primed hPSC samples, calculated from ATAC-seq data using ChromVar. Selected motif families are highlighted.

(E) Projection of RNA-seq data onto published datasets (Tyser et al., 2021; Zheng et al., 2019), showing that, although primed hPSCs and fibroblasts fall within the expected cell types (epiblast and advanced mesoderm, respectively), pdTSCs/ndTSCs/edTSCs are not projected on the amnion cell type.

(F) Projection of RNA-seq data onto a published dataset of *in vivo* placental cells (Vento-Tormo et al., 2018), showing that pdTSCs/ndTSCs/edTSCs cluster with TSC-derived cell lines. DC, dendritic cell; dM, decidual macrophage; dNK, decidual natural killer cell; dS, decidual stromal cell; Endo, endothelial cell; Epi, epithelial glandular cell; fFB, fibroblast; HB, Hofbauer cell; STB, syncytiotrophoblast; VCT, villous CT; EVT, extravillous trophoblast.

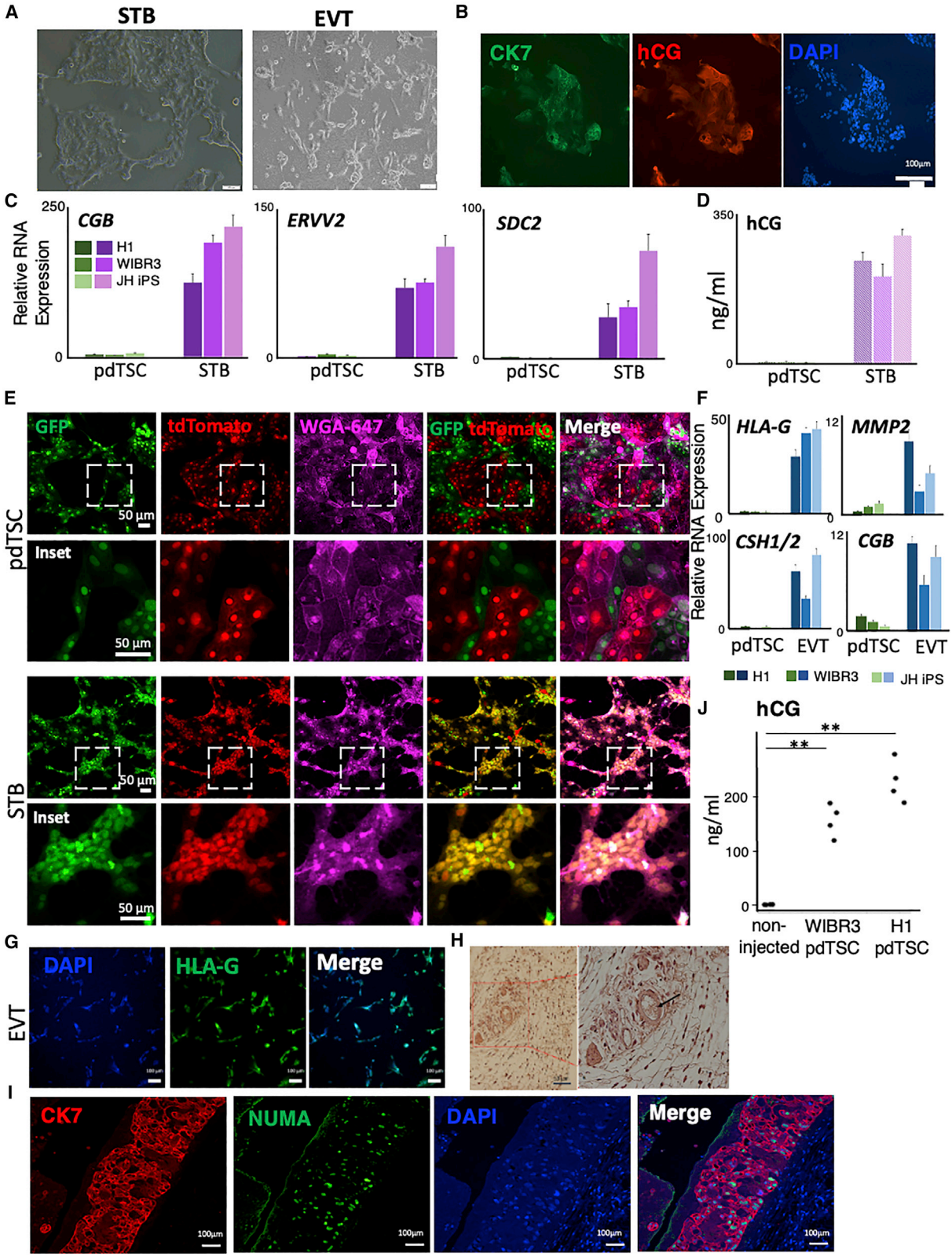


*(legend on next page)*

human placental cells and, therefore, authentically represent TSC lines.

### pdTSCs can differentiate into the main trophoblast lineages and form lesions upon injection into non-obese diabetic (NOD)-severe combined immunodeficiency (SCID) mice

A key property of TSCs is their ability to differentiate into the main trophoblast lineages (STB and EVT) to which they give rise *in vivo*. To test whether our pdTSCs can generate STB, as described previously for edTSCs and ndTSCs (Cinkornpumin et al., 2020; Dong et al., 2020), pdTSCs were treated with a STB differentiation protocol (Okae et al., 2018) and, after 6 days, formed multinucleated syncytium with a typical multinucleated structure (Figure 4A). Strong STB marker upregulation was detected by RT-PCR (*CGB*, *ERVV2*, and *SDC2*) and immunostaining (Figures 4B and 4C), and high levels of hCG protein, which is typically secreted by STB, were identified by ELISA in the medium (Figure 4D). To prove that these multinucleated structures are formed through cell fusion, pdTSCs were marked by constitutive GFP or tdTomato (Figure 4E). GFP- and tdTomato-expressing pdTSCs were mixed and cultured under STB conditions. Although cells that remained in TSC medium formed separate clusters of red and green cells, the multinucleated STB cells expressed both markers, proving that cells underwent fusion (Figure 4E).

To show differentiation of pdTSCs into the EVT lineage, cells were differentiated using a conventional protocol (Okae et al., 2018). The resulting cells expressed high levels of EVT markers such as *HLA-G*, *MMP2*, *CSH1/2*, and *CGB* (Figure 4F) and stained positively for HLA-G protein (Figure 4G). Last, pdTSCs were able to form lesions after injection into mice; H1- and WIBR3-derived pdTSCs were injected into male NOD-SCID mice. After 7 days, 3- to 7-mm lesions were observed (Figure 4H). These lesions had a necrotic middle region surrounded by CK7+ CT-like cells (Figures 4H and 4I). Other cells morphologically resembled STB cells and contained blood-filled lacunae (Figure 4H). To prove that the injected cells are the source of the lesions, the samples were co-stained for the specific human antigen NUMA (Figure 4I). Host mouse serum contained a significant amount of hCG (Figure 4J), in agreement with previous reports (Okae et al., 2018; Turco et al., 2018), indicating that the injected cells retain trophoblast properties.

### Huma naïve PSCs are not more susceptible to generating TSCs than primed hPSCs

Recent reports claim that only naïve human pluripotent cells retain the potential to convert into TSC-like cells (Guo et al., 2021; Dong et al., 2020; Io et al., 2021). Because our results show that primed hPSCs can generate TSCs (Figures 1 and 2), we checked whether cells that generate TSCs are passing transiently through a naïve state. The conversion protocol was therefore applied to WIBR3, H1, and JH iPSC primed hPSC lines, and the expression of naïve markers was measured daily by RT-PCR. No upregulation of naïve markers (*DPPA3*, *TFCP2L1*, *DNMT3L*, *KLF17*, and *KHDC1L*) was detected on any day of the induction process (Figure 5A), indicating that the cells do not pass through some transient, quasi-naïve state during their conversion from primed PSCs.

Because previously published TSC conversion protocols applied TSC-m media directly to naïve human ESCs without using a prior induction step, as devised in our protocol described here (Cinkornpumin et al., 2020; Dong et al., 2020; Io et al., 2021; Guo et al., 2021; Bayerl et al., 2021), we tested the ability of hPSCs to convert into TSCs by applying alternative previously described protocols that do not use an induction step. To test this, TSC-m medium was applied directly to isogenic naïve and primed human GATA3-mCherry reporter cells without the prior induction step. Although the naïve line (expanded in HENSM) induced GATA3-mCherry reporter expression in about 50% of cells after 4 days, primed cells nearly failed

**Figure 4. Formation of the placental lineages STB and EVT from pdTSCs**

(A) Representative images of induced syncytium trophoblast (left) and induced extravillous CT (right), generated from pdTSCs at the end of the 6-day differentiation protocols.

(B) Immunostaining of the STB markers CK7 and hCG in STB cells derived from pdTSCs.

(C) Relative expression of the STB markers *CGB*, *ERVV2*, and *SDC2*, measured by RT-PCR. n = 3 independent experiments.

(D) Levels of hCG secreted hormone, measured by ELISA.

(E) A mixture of GFP- and tdTomato-expressing pdTSCs after treatment with STB differentiation medium (bottom) and without treatment (top). WGA-647 marks the cell membrane.

(F) Relative expression of the EVT markers HLA-G, MMP2, CSH1/2, and CGB, measured by RT-PCR. n = 3 independent experiments.

(G) Immunostaining of the EVT marker HLA-G in EVT cells derived from pdTSCs.

(H) H&E staining of the pdTSC lesions formed in male NOD-SCID mice. An arrow indicates blood-filled lacunae surrounded by trophoblast cells. A red dotted line highlights the enlarged inset on the right.

(I) Immunostaining for CK7 and NUMA in pdTSC-formed lesions.

(J) hCG levels in serum of a host male mouse that was injected with pdTSCs derived from WIBR3 and H1 hESCs or a non-injected control. Student's t test, $^{**}p < 0.0012$. n = 4 independent experiments.

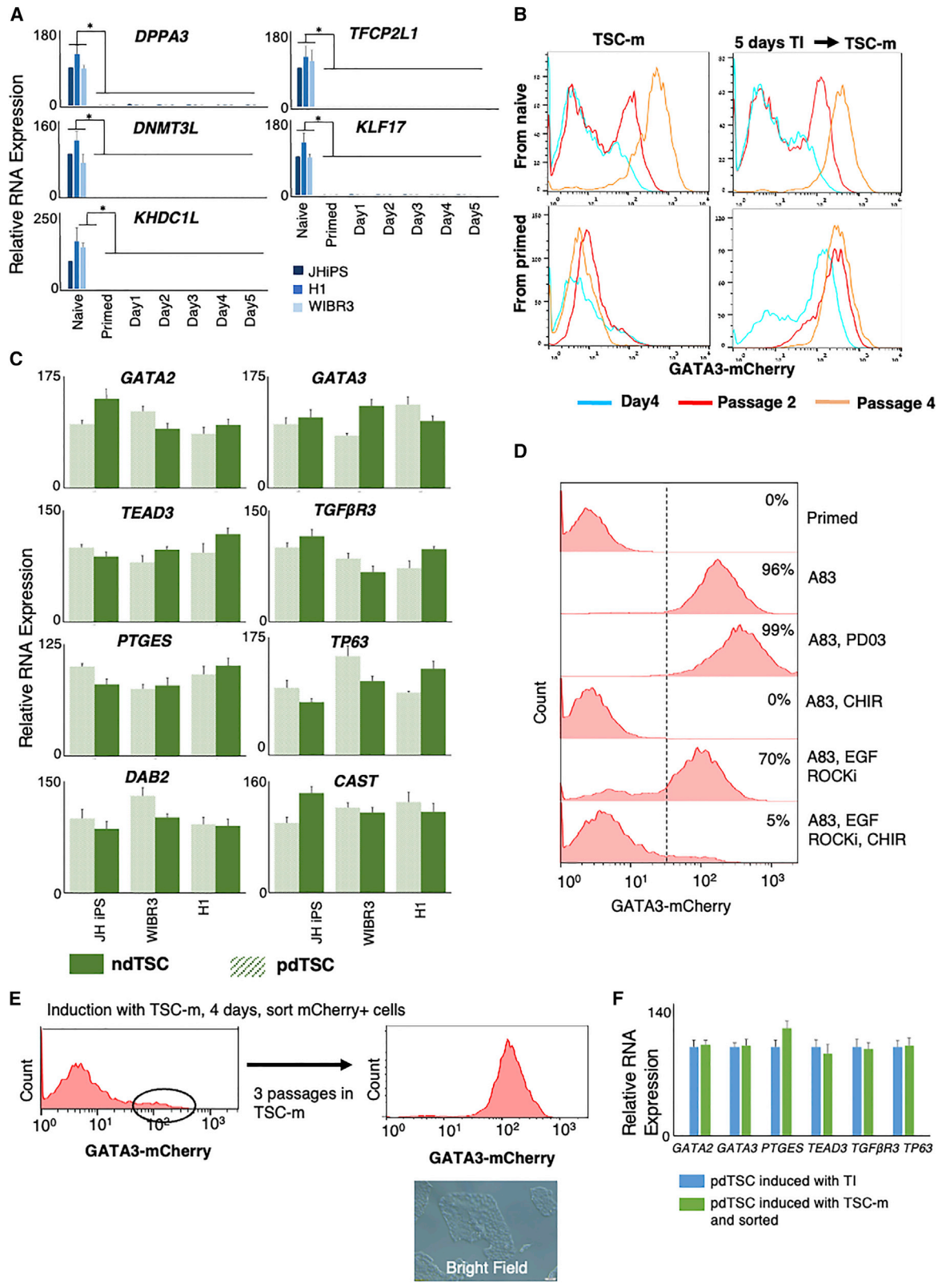


*(legend on next page)*

to do so (Figure 5B, left). These results corroborate the findings published previously by others (Dong et al., 2020; Guo et al., 2021).

Next, naïve and primed hPSCs were differentiated into TSCs using 5 days in TI medium and shifting to TSC-m medium (Figure 5B, right). For naïve cells, the conversion kinetics were similar when using a protocol with or without induction step with TI, forming an up to 98% GATA3-mCherry+ population by passage 4. The conversion of naïve cells with an induction step or by direct TSC-m medium application was slower compared with primed cells; naïve cells established homogeneous ndTSC populations by passages 3–5, whereas TSCs derived from primed cells showed uniform *GATA3* expression and *bona fide* TSC morphology already by passage 2 (Figures 1D, 1E, and 5B). These slower conversion kinetics for naïve ESCs are consistent with results reported by Dong et al. (2020), although different naïve human ESC conditions were used in both studies. These results indicate that the inability or difficulty to obtain human TSCs is not an inherent property of the human primed state but rather reflects a technical factor: suboptimal differentiation protocols that were not customized for human primed cells, which need an induction step, as delineated here (Figure 1B).

Naïve hPSC lines from 3 different backgrounds were converted into TSCs by direct TSC-m medium application, showing similar marker expression compared with their counterparts converted from primed lines (Figure 5C). Some subtle differences in expression were observed between ndTSCs and pdTSCs, such as upregulation of DPPA4 and ERK signaling (e.g., *SNAI2* and *TNC*) transcripts in ndTSCs (Figure S4A). ndTSCs were successfully differentiated into STB and EVT cells (Figures S4B–S4D). Overall, the high similarity between the profiles proves that the induced TSCs show an authentic TSC-like signature, regardless of the origin of the cells from which they were derived.

## Inclusion of GSK3i derails human primed PSCs away from the TSC lineage

The above results support the conclusion that one of the components in TSC-m, which is not found in TI, negatively influences the ability of primed hPSCs to successfully convert into TSCs. When TSC-m medium was applied directly to primed hPSCs and in accordance with previous reports (Dong et al., 2020; Guo et al., 2021), the cells generated GATA3− cultures that showed homogeneous morphology and proliferated rapidly for at least 20 passages. However, these cells did not express trophoblast markers but a mix of neuronal lineage commitment markers, like *PAX6* and *SOX1* (Figures S5A and S5B).

We therefore attempted to induce TSCs in primed cell cultures by applying TSC-m medium with separate addition of the TSC-m components on TI-based medium and realized that addition of CHIR, a GSK3 inhibitor that leads to WNT activation, ablates induction of GATA3+ cells from primed PSCs and that its omission from TSC-m medium permits derivation of TSC lines from primed cells even in the presence of EGF and ROCK inhibition without the need for a TI step (Figure 5D). Direct application of TSC-m medium on primed GATA3-mCherry cells did yield a small GATA3+ fraction. After sorting out these mCherry+ cells, we were able to establish *bona fide* TSC lines from hPSCs even when GSK3i was included (Figures 5E and 5F). In summary, the inclusion of GSK3i in TSC media used in previous studies (Dong et al., 2020; Guo et al., 2021; Io et al., 2021) likely underlies their reproted difficulty in isolating TSCs from human primed PSCs, which turned out to be a merely technical inability.

## Nuclear YAP is necessary and sufficient for conversion of human PSCs into TSCs

YAP translocation to the nucleus in morula outer cells is a crucial event in induction of mammalian embryo TE (Rossant and Tam, 2009). Induced nuclear localization of the YAP cofactor TEAD4 is sufficient to convert mouse naïve ESCs into TSCs (Nishioka et al., 2009). We tested whether constitutively active YAP2-5SA (YAP*) (Zhao et al., 2007) gene overexpression can induce TSCs from primed hPSCs. Primed hPSCs were electroporated with YAP*-IRES-CFP or with a control IRES-CFP construct (Figure 6A) and seeded into N2B27 medium without a TGF-β inhibitor. After

**Figure 5. Derivation of TSCs from HENSM naïve and primed hPSCs**

(A) Relative expression of the naïve hPSC markers *DPPA3*, *DNMT3L*, *KHDC1L*, *TFCP2L1*, and *KLF17* in naïve (HENSM) and primed hPSCs and during 5 days in TI medium, measured by RT-PCR. Student's t test, *p < 0.05. n = 3 independent experiments.

(B) Conversion kinetics of naïve and primed GATA3-mCherry hPSCs by direct application of TSC-m medium (left) or 5-days treatment with TI medium followed by TSC-m medium (right).

(C) Relative expression of TSC markers, measured in induced TSCs that were derived from HENSM naïve or primed hPSCs of the indicated backgrounds (n = 4 independent experiments).

(D) GATA3-mCherry-primed hPSCs treated with N2B27 with the indicated compounds added, showing abrogation of GATA3 expression by CHIR. Note a 5% GATA3-mCherry fraction in the cells treated with TSC-m (bottom panel).

(E) Bottom panel from (D). The mCherry+ fraction is sorted out and gives rise to *bona fide* TSC culture.

(F) Relative expression of TSC markers, measured in pdTSCs that were maintained in TI medium (blue) or pdTSC that were sorted out as explained in (E) (green) (n = 4 independent experiments).

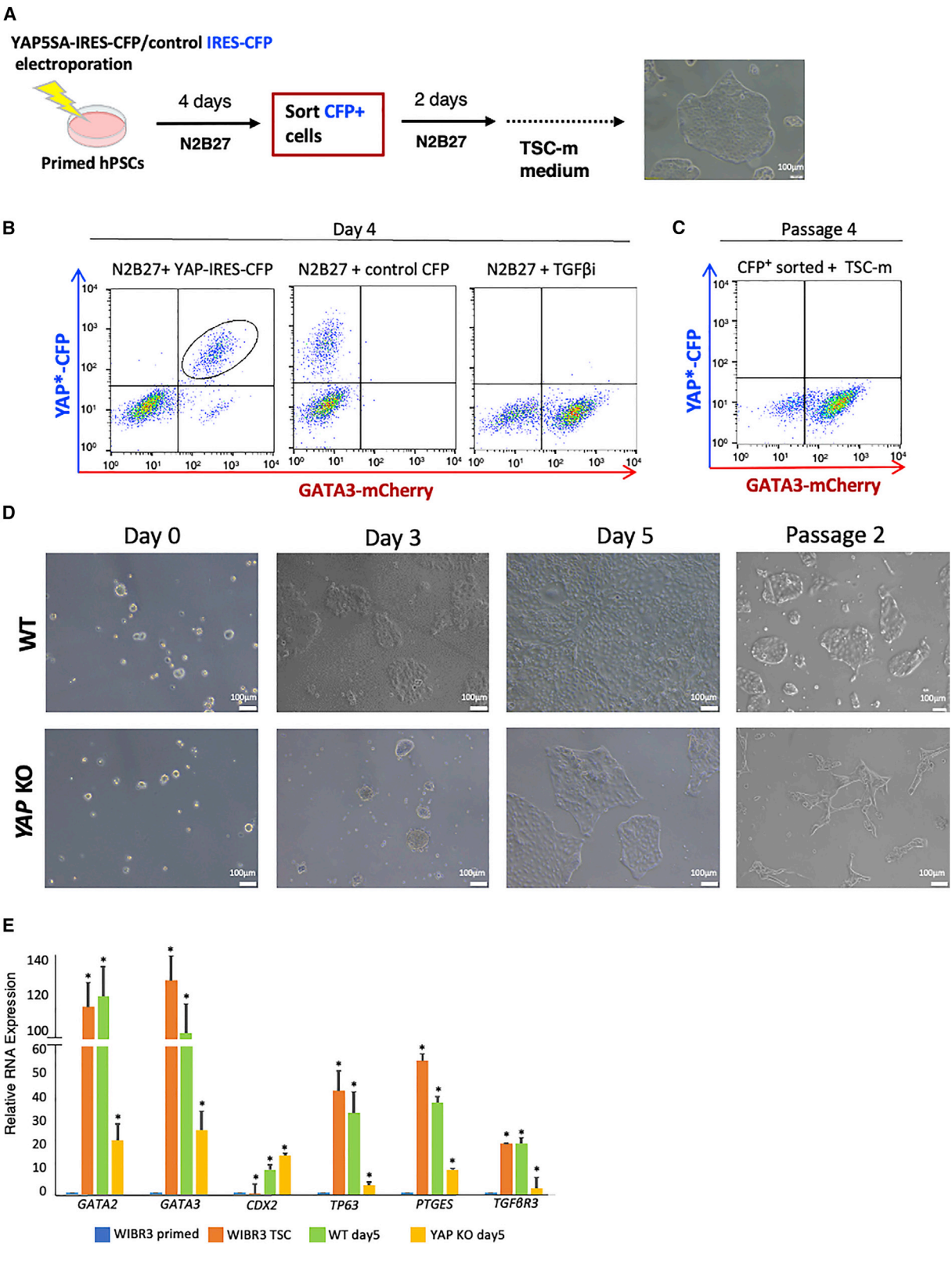


*(legend on next page)*

4 days, the control cells did not express the GATA3 reporter, whereas in cultures transfected with YAP*, nearly all cells that expressed CFP also expressed mCherry (Figure 6B). A minor CFP− mCherry+ fraction could also be observed, probably indicating cells that were induced by transfected YAP* but have lost the expression plasmid by the time of the measurement. This result indicates that upregulation of YAP signaling alone is sufficient to initiate conversion to TSCs under minimal basal conditions.

Four days after electroporation, the CFP+ GATA3+ population was sorted, seeded back to N2B27 medium for 2 days, and then changed to TSC-m medium. The cells gave rise to self-renewing cultures with TSC morphology (Figure 6A). The experiment was repeated with other primed hPSC lines (H1 and JH iPSC) that do not carry the GATA3 reporter. Here the CFP+ cells were sorted out and gave rise to pdTSC cultures. CFP+ cells could not be detected by passages 3–4, indicating that YAP* overexpression was indeed transient (Figure 6C). All YAP-induced TSC lines were readily differentiated into EVT and STB lineages, as demonstrated by marker expression (Figures S5C–S5E), proving that YAP signaling alone is sufficient to induce *bona fide* TSCs with adequate functional capabilities.

Next, to check whether YAP is essential for TSC generation, the *YAP* gene was knocked out in WIBR3 cells (Figures S5F–S5H). TI medium was applied on *YAP* knockout (KO) cells, and although, during the first 5 days, they started to show a TSC-like morphology, cell growth was retarded compared with the wild-type control (Figure 6D). When the cells were passaged on day 5 to TSC-m medium, they stopped proliferating and eventually died. RT-PCR on the samples collected on day 5 show that some TSC markers, such as *GATA2*, *GATA3*, *PTGES*, and *TGFβR3* were only mildly upregulated, whereas *TP63* was not induced (Figure 6E).

## DISCUSSION

In this study, we developed a robust protocol for conversion of primed hPSCs into TSC lines, highly similar in features to TSC lines derived from early placenta and preimplantation blastocyst and TSCs differentiated from naïve hPSCs. These pdTSCs can be derived robustly from hPSCs of different origins, including multiple established hESC lines and iPSCs. The relative ease of applying this protocol to primed iPSC may open new opportunities to investigate placental disorders *in vitro*. pdTSCs can differentiate into the main human trophoblast lineages EVT and STB, and they can form KRT7+ lesions in NOD-SCID mice while increasing the concentration of hCG in injected male mouse blood. By performing ATAC-seq and RNA-seq, we demonstrated remarkable transcriptional and epigenetic similarity between pdTSC and all previously generated TSC lines.

Previous reports have described derivation of TSC lines from naïve hPSCs by simply switching the growth medium from ESC to TSC conditions (Cinkornpumin et al., 2020; Dong et al., 2020). Here we confirmed that transcriptional and epigenetic profiles of ndTSCs and primed hPSC-derived TSCs are highly similar. However, efficient and rapid conversion of primed PSCs into TSCs optimally requires usage of an induction stage. Application of TSC-m medium that contains a GSK3 inhibitor directly on primed cells results in rapid differentiation into non-trophoblast somatic lineages (Figure S6). Despite this, we observed, in accordance with Wei et al. (2021), that even direct addition of TSC medium to primed cells does give rise to a small GATA3+ fraction from which a normal TSC line can be established (Figures 5E and 5F). We conclude that application of CHIR, EGF, and TGF-β inhibitor-containing medium to primed, but not naïve, hPSCs gives rise to the trophoblast and neural lineage; the latter is capable of more rapid proliferation and quickly overgrows the TSCs.

Wnt/β-catenin signaling is an essential player in ESC regulation. Although the mouse ESC naïve state is supported by nuclear β-catenin activation, human naïve conditions require Tankyrase/Wnt suppression for their induction and maintenance (Bayerl et al., 2021). CHIR or Wnt ligands are indispensable components of many hPSC differentiation protocols. A Pax6+Sox1+ population readily emerged in TSC conditions from primed cells but was not

**Figure 6. Role of nuclear YAP in human TSC derivation and maintenance**

(A) YAP* (YAP2-5SA mutant) overexpression experimental scheme.

(B) GATA3-mCherry reporter and CFP expression in cells treated with N2B27 medium for 4 days. Left: cells with the YAP*-IRES-CFP construct. Center: cells with empty vector (negative control). Right: cells treated with TGF-β inhibitor (TGFβi) (positive control). The indicated $mCherry^{+}CFP^{+}$ fraction was sorted and maintained in TSC-m medium.

(C) The sorted fraction state after 4 passages. Note that CFP is not expressed at this time point, indicating the absence of exogenous YAP*.

(D) Conversion of WIBR3 wild-type (WT) primed hPSCs (top panel) and $YAP^{-/-}$ hPSCs. Note the TSC-like morphology on day 5 in $YAP^{-/-}$ cells; however, they stop growing and degrade at passage 2.

(E) RT-PCR detection of TSC markers of WIBR3 WT and $YAP^{-/-}$ primed hPSCs after 5 days in TI medium compared with primed hPSCs and established pdTSCs (both WIBR3) at passage 10. Note the moderate upregulation of *GATA2*, *GATA3*, *PTGES*, and *TGFβR3* and strong upregulation of *CDX2*. n = 3 independent experiments). Student's t test, *p < 0.05 compared with primed.

visible in converting naïve hPSCs. Our findings might indicate an intriguing difference between naïve and primed hPSC response to β-catenin activation that deserves further investigation. Our results supplement ones published recently (Wei et al., 2021), where addition of BMP4 to CHIR-containing TSC medium makes it possible to derive induced TSCs from primed cells. In our hands, subtraction of CHIR from TSC medium also makes conversion of primed hPSCs to TSCs possible, suggesting a possible mutual suppression between WNT and BMP4 in this cell fate choice.

HIPPO signaling inhibition leading to YAP translocation to the nuclei of the outer cells of the mouse early blastocyst is an essential trigger for trophoblast lineage specification (Rossant and Tam, 2009). Upregulation of the YAP cofactor Tead4 gene in mouse naïve ESCs converts them to TSCs (Nishioka et al., 2009). YAP protein shows nuclear localization in TSCs and prevents CTs from differentiation (Dong et al., 2020; Meinhardt et al., 2020). Here we confirmed that transient overexpression of constitutively active YAP in primed ESCs replaces TGF-β inhibition in the conversion protocol. *YAP* KO hPSCs do not give rise to TSC lines and are lost by the second passage after induction with a TGF-β inhibitor. Some TSC-specific markers do show some upregulation upon TGF-β inhibition in *YAP* KO hPSCs, possibly because of the presence of another HIPPO signaling effector, TAZ. To check whether at least some part of the trophoblast program can be induced in complete absence of HIPPO signaling effectors, we attempted to make *YAP/TAZ* double KO hPSCs but failed to do so, likely because such double KO cells do not survive under human primed conditions. Our results support the conclusion that YAP signaling is sufficient for TSC program induction and necessary for TSC maintenance.

Conversion of mouse ESCs to TSCs is also well established and commonly involves using transient exogenous *Cdx2* transgenes (Nishioka et al., 2009; Niwa et al., 2005). This conversion works from the naïve ESC state but not from the primed one (Blij et al., 2015; Tarazi et al., 2022). This result is believed to reflect higher developmental proximity between naïve ESCs and the trophoblast lineage because naïve ES cells model preimplantation ICM/epiblast, whereas primed cells are more similar to early post-implantation epiblast (Weinberger et al., 2016). The straightforward conversion of human primed ESCs to TSCs is a counterintuitive example of *trans*-differentiation between developmentally separated lineages and demonstrates a striking difference between human and mouse stem cells states. However, all human TSC lines derived so far correspond transcriptionally to post-implantation stage trophoblasts ( Dong et al., 2020; Okae et al., 2018), which could explain why human primed PSCs are still amenable to give rise to such cells. We cannot exclude the possibility that the ability of primed PSCs to convert into TSCs is an *in vitro*-specific phenomenon that does not occur *in vivo*. It is possible that human naïve PSCs might be more prone to give rise to TSCs that correspond to preimplantation stages in the future because conditions for isolating such TSCs have not been defined so far. Finally, the generation of extra-embryonic TSCs from human naïve and primed PSCs may prove useful for future attempts to *in vitro* generate advanced human stem-cell-derived embryo models (SEMs) solely from stem cells to model early human embryo development from gastrulation to organogenesis *ex utero*, as we recently showed in mice (Tarazi et al., 2022).

## EXPERIMENTAL PROCEDURES

### Resource availability

#### *Materials availability*

Unique reagents generated in this study are available from the lead contact with a materials transfer agreement.

#### *Lead contact*

Further information and requests for resources and reagents should be directed to the lead contact, J.H.H. (jacob.hanna@weizmann.ac.il).

### Culture of human naïve and primed ESCs and iPSCs

Naïve human ESCs and iPSCs were cultured in a 5% $O_2$, 5% $CO_2$, 37°C incubator on Matrigel (growth factor reduced)-coated plates under standardized HENSM conditions (based on Bayerl et al., 2021) to accommodate a larger variety of human ESC and iPSC lines from different genetic backgrounds with daily medium exchange. HENSM contained 235 mL Neurobasal (Thermo Fisher Scientific, 21103049), 235 mL DMEM-F12 without HEPES (Thermo Fisher Scientific, 21331020), 5 mL N2 supplement (prepared in house, or 5 mL of Invitrogen–Thermo Fisher Scientific 17502-048), 5 mL GlutaMAX (Thermo Fisher Scientific, 35050061), 1% (5 mL) non-essential amino acids (BI, 01-340-1B), 1% (5 mL) penicillin-streptomycin (BI, 03-031-1B), 1% (5 mL) sodium pyruvate (BI, 03-042-1B), 10 mL B27 supplement (Invitrogen, 17504-044), 1 mL Geltrex (Invitrogen, A1413202), 50 μg/mL vitamin C (L-ascorbic acid 2-phosphate, Sigma, A8950), 100 μM 2-mercaptoethanol (optional, 1 mL of 50 mM ready-made solution, Invitrogen, 31350010), 10 ng/mL recombinant human LIF (PeproTech, 300-05, or made in house), MEKi/ERKi (PD0325901, 1 μM, Axon Medchem, 1408), WNTi/TNKi (XAV939, 2 μM, Axon Medchem, 1527), PKCi (Go6983, 2 μM, Axon Medchem, 2466), ROCKi (Y27632, 1.2 μM, Axon Medchem, 1683), SRCi (CGP77675, 1 μM, Axon Medchem, 2097), and human Activin A (5 ng/mL, PeproTech, 120-14E).

Some lines required slightly higher inhibition of fibroblast growth factor (FGF)/MEK/ERK signaling to achieve a more homogeneous dome-like morphology (e.g., WIBR3 hESCs, RUES2 hESCs), which could be done by increasing MEKi/ERKi (PD0325901) from 1 μM to 1.2 μM or adding 0.05 μM or 0.1 μM FGFRi (PD173074, Axon Medchem, 1673) to the condition mix above. These changes can be done after initial conversion with

the basic HENSM composition indicated above (Figure 2F), and after a couple of passages, one can gradually increase MEKi or FGFRi, as suggested above. Similar results were obtained in early stages of this study when using the original HENSM conditions as previously described in (Bayerl et al., 2021).

All cells were routinely passaged with 0.05% trypsin or TrypLE. For primed hPSCs, 10 μM ROCKi was added 24 h before and after passaging, and for naïve PSCs, 5 μM ROCKi was added for 24 h after passaging.

Primed human PSCs were cultured on irradiated MEFs in DMEM-F12 (Invitrogen, 10829) supplemented with 15% KO serum replacement (Invitrogen, 10828-028), 1 mM GlutaMAX (Invitrogen), 1% non-essential amino acids (BI, 01-340-1B), 1% penicillin-streptomycin (BI, 03-031-1B), and 8 ng/mL bFGF (PeproTech) under 20% $O_2$, 5% $CO_2$ conditions.

Additional experimental procedures are included in the supplemental information.

## DATA AND CODE AVAILABILITY

All RNA-seq and ATAC-seq data reported in this study have been deposited in Gene Expression Omnibus (https://www.ncbi.nlm.nih.gov/geo/). The accession number for the data reported in this paper is GEO: GSE213164. Software/packages used to analyze the dataset are freely or commercially available.

## SUPPLEMENTAL INFORMATION

Supplemental information can be found online at https://doi.org/10.1016/j.stemcr.2022.09.008.

## AUTHOR CONTRIBUTIONS

S.V. conceived the idea for this project, designed and conducted the experiments, and wrote the manuscript. T.S. conducted computational analyses of the data. J.B., A.A.-C., and B.O. assisted with immunohistochemistry experiments, D.S. generated the ATAC-seq library. Y.S. assisted with the ELF5 methylation experiment. S.T. and J.H.H standardized HENSM conditions across a large number of human ESC and iPSC lines from different genetic backgrounds. N.N. supervised and conducted computational analyses of the data and wrote the manuscript. J.H.H conceived the idea for this project, supervised data analysis, and wrote the manuscript.

## ACKNOWLEDGMENTS

We thank T. Arima (Department of Informative Genetics, Tohoku University Graduate School of Medicine, Senai, Japan) for sharing their published embryo derived human trophoblast stem cell lines. This work was funded by Pascal and Ilana Mantoux, the Nella and Leon Benoziyo Center for Neurological Diseases, the David and Fela Shapell Family Center for Genetic Disorders Research, the Kekst Family Institute for Medical Genetics, the Helen and Martin Kimmel Institute for Stem Cell Research, Flight Attendant Medical Research Institute (FAMRI), the Dr. Beth Rom-Rymer Stem Cell Research Fund, the Edmond de Rothschild Foundations, the Zantker Charitable Foundation, the Estate of Zvia Zeroni, the European Research Council (ERC-CoG; CELLNAIVETY – 726497), the Israel Science Foundation (ISF), Minerva, Research Professorship by the Israel Cancer Research Fund (ICRF), and BSF. We thank the Weizmann Institute management and board for providing critical financial and infrastructural support.

## CONFLICT OF INTERESTS

J.H.H. has submitted patent applications relevant to the findings reported here, related to generation of mammalian synthetic embryoid models, and is a chief scientific advisor of Renewal Bio Ltd., which has licensed technologies described here.

Received: April 25, 2022
Revised: September 20, 2022
Accepted: September 21, 2022
Published: October 20, 2022

## REFERENCES

Amita, M., Adachi, K., Alexenko, A.P., Sinha, S., Schust, D.J., Schulz, L.C., Roberts, R.M., and Ezashi, T. (2013). Complete and unidirectional conversion of human embryonic stem cells to trophoblast by BMP4. Proc. Natl. Acad. Sci. USA *110*, E1212–E1221. https://doi.org/10.1073/pnas.1303094110.

Bayerl, J., Ayyash, M., Shani, T., Manor, Y.S., Gafni, O., Massarwa, R., Kalma, Y., Aguilera-Castrejon, A., Zerbib, M., Amir, H., et al. (2021). Principles of signaling pathway modulation for enhancing human naïve pluripotency induction. Cell Stem Cell *28*, 1549–1565.e12. https://doi.org/10.1016/j.stem.2021.04.001.

Blij, S., Parenti, A., Tabatabai-Yazdi, N., and Ralston, A. (2015). Cdx2 efficiently induces trophoblast stem-like cells in naïve, but not primed, pluripotent stem cells. Stem Cells Dev. *24*, 1352–1365. https://doi.org/10.1089/scd.2014.0395.

Cinkornpumin, J.K., Kwon, S.Y., Guo, Y., Hossain, I., Sirois, J., Russett, C.S., Tseng, H.W., Okae, H., Arima, T., Duchaine, T.F., et al. (2020). Naïve human embryonic stem cells can give rise to cells with a trophoblast-like transcriptome and methylome. Stem Cell Rep. *15*, 198–213. https://doi.org/10.1016/j.stemcr.2020.06.003.

Dong, C., Beltcheva, M., Gontarz, P., Zhang, B., Popli, P., Fischer, L.A., Khan, S.A., Park, K.M., Yoon, E.J., Xing, X., et al. (2020). Derivation of trophoblast stem cells from naïve human pluripotent stem cells. Elife *9*, e52504. https://doi.org/10.7554/eLife.52504.

Gerri, C., McCarthy, A., Alanis-Lobato, G., Demtschenko, A., Bruneau, A., Loubersac, S., Fogarty, N.M.E., Hampshire, D., Elder, K., Snell, P., et al. (2020). Initiation of a conserved trophectoderm program in human, cow and mouse embryos. Nature *587*, 443–447. https://doi.org/10.1038/s41586-020-2759-x.

Guo, G., Stirparo, G.G., Strawbridge, S.E., Spindlow, D., Yang, J., Clarke, J., Dattani, A., Yanagida, A., Li, M.A., Myers, S., et al. (2021). Human naïve epiblast cells possess unrestricted lineage potential. Cell Stem Cell *28*, 1040–1056.e6. https://doi.org/10.1016/j.stem.2021.02.025.

Gafni, O., Weinberger, L., Mansour, A.A., Manor, Y.S., Chomsky, E., Ben Yosef, D., Kalma, Y., Viukov, S., Maza, I., Zviran, A., et al. (2013). Derivation of novel human ground state naïve pluripotent stem cells. Nature *504*, 282–286. https://doi.org/10.1038/nature12745.

Guo, G., von Meyenn, F., Rostovskaya, M., Clarke, J., Dietmann, S., Baker, D., Sahakyan, A., Myers, S., Bertone, P., Reik, W., et al. (2017). Epigenetic resetting of human pluripotency. Development *144*, 2748–2763. https://doi.org/10.1242/dev.146811.

Hemberger, M., Udayashankar, R., Tesar, P., Moore, H., and Burton, G.J. (2010). ELF5-enforced transcriptional networks define an epigenetically regulated trophoblast stem cell compartment in the human placenta. Hum. Mol. Genet. *19*, 2456–2467. https://doi.org/10.1093/hmg/ddq128.

Io, S., Kabata, M., Iemura, Y., Semi, K., Morone, N., Minagawa, A., Wang, B., Okamoto, I., Nakamura, T., Kojima, Y., et al. (2021). Capturing human trophoblast development with naïve pluripotent stem cells in vitro. Cell Stem Cell *28*, 1023–1039.e13. https://doi.org/10.1016/j.stem.2021.03.013.

James, J.L., Carter, A.M., and Chamley, L.W. (2012). Human placentation from nidation to 5 weeks of gestation. Part I: what do we know about formative placental development following implantation? Placenta *33*, 327–334. https://doi.org/10.1016/j.placenta.2012.01.020.

Jang, Y.J., Kim, M., Lee, B.K., and Kim, J. (2022). Induction of human trophoblast stem-like cells from primed pluripotent stem cells. Proc. Natl. Acad. Sci. USA *119*, e2115709119. https://doi.org/10.1073/pnas.2115709119.

Latos, P.A., and Hemberger, M. (2016). From the stem of the placental tree: trophoblast stem cells and their progeny. Development *143*, 3650–3660. https://doi.org/10.1242/dev.133462.

Lengner, C.J., Gimelbrant, A.A., Erwin, J.A., Cheng, A.W., Guenther, M.G., Welstead, G.G., Alagappan, R., Frampton, G.M., Xu, P., Muffat, J., et al. (2010). Derivation of pre-X inactivation human embryonic stem cells under physiological oxygen concentrations. Cell *141*, 872–883. https://doi.org/10.1016/j.cell.2010.04.010.

Liu, X., Ouyang, J.F., Rossello, F.J., Tan, J.P., Davidson, K.C., Valdes, D.S., Schröder, J., Sun, Y.B.Y., Chen, J., Knaupp, A.S., et al. (2020). Reprogramming roadmap reveals route to human induced trophoblast stem cells. Nature *586*, 101–107. https://doi.org/10.1038/s41586-020-2734-6.

Meinhardt, G., Haider, S., Kunihs, V., Saleh, L., Pollheimer, J., Fiala, C., Hetey, S., Feher, Z., Szilagyi, A., Than, N.G., and Knöfler, M. (2020). Pivotal role of the transcriptional co-activator YAP in trophoblast stemness of the developing human placenta. Proc. Natl. Acad. Sci. USA *117*, 13562–13570. https://doi.org/10.1073/pnas.2002630117.

Mischler, A., Karakis, V., Mahinthakumar, J., Carberry, C.K., San Miguel, A., Rager, J.E., Fry, R.C., and Rao, B.M. (2021). Two distinct trophectoderm lineage stem cells from human pluripotent stem cells. J. Biol. Chem. *296*, 100386. https://doi.org/10.1016/j.jbc.2021.100386.

Niakan, K.K., Han, J., Pedersen, R.A., Simon, C., and Pera, R.A.R. (2012). Human pre-implantation embryo development. Development *139*, 829–841. https://doi.org/10.1242/dev.060426.

Nishioka, N., Inoue, K.i., Adachi, K., Kiyonari, H., Ota, M., Ralston, A., Yabuta, N., Hirahara, S., Stephenson, R.O., Ogonuki, N., et al. (2009). The Hippo signaling pathway components Lats and Yap pattern Tead4 activity to distinguish mouse trophectoderm from inner cell mass. Dev. Cell *16*, 398–410. https://doi.org/10.1016/j.devcel.2009.02.003.

Niwa, H., Toyooka, Y., Shimosato, D., Strumpf, D., Takahashi, K., Yagi, R., and Rossant, J. (2005). Interaction between Oct3/4 and Cdx2 determines trophectoderm differentiation. Cell *123*, 917–929. https://doi.org/10.1016/j.cell.2005.08.040.

Okae, H., Toh, H., Sato, T., Hiura, H., Takahashi, S., Shirane, K., Kabayama, Y., Suyama, M., Sasaki, H., and Arima, T. (2018). Derivation of human trophoblast stem cells. Cell Stem Cell *22*, 50–63.e6. https://doi.org/10.1016/j.stem.2017.11.004.

Petropoulos, S., Edsgärd, D., Reinius, B., Deng, Q., Panula, S.P., Codeluppi, S., Plaza Reyes, A., Linnarsson, S., Sandberg, R., and Lanner, F. (2016). Single-cell RNA-seq reveals lineage and X chromosome dynamics in human preimplantation embryos. Cell *165*, 1012–1026. https://doi.org/10.1016/j.cell.2016.03.023.

Rossant, J., and Tam, P.P.L. (2009). Blastocyst lineage formation, early embryonic asymmetries and axis patterning in the mouse. Development *136*, 701–713. https://doi.org/10.1242/dev.017178.

Soncin, F., Khater, M., To, C., Pizzo, D., Farah, O., Wakeland, A., Arul Nambi Rajan, K., Nelson, K.K., Chang, C.W., Moretto-Zita, M., et al. (2018). Comparative analysis of mouse and human placentae across gestation reveals species-specific regulators of placental development. Development *145*, dev156273. https://doi.org/10.1242/dev.156273.

Soncin, F., Morey, R., Bui, T., Requena, D.F., Cheung, V.C., Kallol, S., Kittle, R., Jackson, M.G., Farah, O., Dumdie, J., et al. (2022). Derivation of functional trophoblast stem cells from primed human pluripotent stem cells. Stem Cell Rep. *17*, 1303–1317. https://doi.org/10.1016/j.stemcr.2022.04.013.

Tarazi, S., Aguilera-Castrejon, A., Joubran, C., Ghanem, N., Ashouokhi, S., Roncato, F., Wildschutz, E., Haddad, M., Oldak, B., Gomez-Cesar, E., et al. (2022). Post-gastrulation synthetic embryos generated ex utero from mouse naïve ESCs. Cell *185*, 3290–3306.e25. https://doi.org/10.1016/j.cell.2022.07.028.

Turco, M.Y., Gardner, L., Kay, R.G., Hamilton, R.S., Prater, M., Hollinshead, M.S., McWhinnie, A., Esposito, L., Fernando, R., Skelton, H., et al. (2018). Trophoblast organoids as a model for maternal-fetal interactions during human placentation. Nature *564*, 263–267. https://doi.org/10.1038/s41586-018-0753-3.

Turco, M.Y., and Moffett, A. (2019). Development of the human placenta. Development *146*, dev163428. https://doi.org/10.1242/dev.163428.

Tyser, R.C.V., Mahammadov, E., Nakanoh, S., Vallier, L., Scialdone, A., and Srinivas, S. (2021). Single-cell transcriptomic characterization of a gastrulating human embryo. Nature *600*, 285–289. https://doi.org/10.1038/s41586-021-04158-y.

Vento-Tormo, R., Efremova, M., Botting, R.A., Turco, M.Y., Vento-Tormo, M., Meyer, K.B., Park, J.E., Stephenson, E., Polański, K., Goncalves, A., et al. (2018). Single-cell reconstruction of the early maternal-fetal interface in humans. Nature *563*, 347–353. https://doi.org/10.1038/s41586-018-0698-6.

Wei, Y., Wang, T., Ma, L., Zhang, Y., Zhao, Y., Lye, K., Xiao, L., Chen, C., Wang, Z., Ma, Y., et al. (2021). Efficient derivation of human trophoblast stem cells from primed pluripotent stem cells. Sci. Adv. *7*, eabf4416. https://doi.org/10.1126/sciadv.abf4416.

Weinberger, L., Ayyash, M., Novershtern, N., and Hanna, J.H. (2016). Dynamic stem cell states: naïve to primed pluripotency in rodents and humans. Nat. Rev. Mol. Cell Biol. *17*, 155–169. https://doi.org/10.1038/nrm.2015.28.

Ying, Q.L., Wray, J., Nichols, J., Batlle-Morera, L., Doble, B., Woodgett, J., Cohen, P., and Smith, A. (2008). The ground state of embryonic stem cell self-renewal. Nature *453*, 519–523. https://doi.org/10.1038/nature06968.

Zhao, B., Wei, X., Li, W., Udan, R.S., Yang, Q., Kim, J., Xie, J., Ikenoue, T., Yu, J., Li, L., et al. (2007). Inactivation of YAP oncoprotein by the Hippo pathway is involved in cell contact inhibition and tissue growth control. Genes Dev. *21*, 2747–2761. https://doi.org/10.1101/gad.1602907.

Zhao, C., Reyes, A.P., Schell, J.P., Weltner, J., Ortega, N., Zheng, Y., Björklund, Å.K., Rossant, J., Fu, J., Petropoulos, S., and Lanner, F. (2021). Reprogrammed iBlastoids contain amnion-like cells but not trophectoderm. Preprint at bioRxiv. https://doi.org/10.1101/2021.05.07.442980.

Zheng, Y., Xue, X., Shao, Y., Wang, S., Esfahani, S.N., Li, Z., Muncie, J.M., Lakins, J.N., Weaver, V.M., Gumucio, D.L., and Fu, J. (2019). Controlled modelling of human epiblast and amnion development using stem cells. Nature *573*, 421–425. https://doi.org/10.1038/s41586-019-1535-2.